International Journal for Scientific Research (IJSR)

المجلة الدولية للبحوث العلمية

Vol. (4), No. (7) July 2025 الإصدار (4)، العدد (7)

Comparative Analysis of Classification Techniques for Water Body Extraction from TerraSAR-X Satellite Imagery

Sumaya Falih Hasan

Department of Surveying Engineering Techniques, Technical Engineering College of Kirkuk, Northern Technical University, Kirkuk, Iraq

sumaya.h.falih@ntu.edu.iq

Abstract

This paper explores different classification algorithms for the extraction of water bodies within TerraSAR-X polarimetric imagery with a case study situated in the Atchafalaya delta region of Louisiana. Various classification techniques, such as Maximum Likelihood Classification (MLH), Mahalanobis Distance (MHD), Minimum Distance (MND), Neural Networks (NN) and Support Vector Machines (SVM) were evaluated. Each approach was tested on its capability to delimit water in synthetic aperture radar (SAR) imagery despite environmental influences, such as wind speed effects and the emergence of vegetation.

The outcomes indicated that the conventional technique including MLH, MHD and MND had difficulty for accurate results where MLH achieved an overall accuracy of the 85.73% and Kappa of 0.7594, while MHD as well as MND also showed the results along the same line with the accuracy as 98.5% and Kappa of 0.97. The comparison shows that the NN and SVM methods are highly competitive compared with other methods, the NN method reached 99.57% accuracy and 0.9913 Kappa value, whereas SVM presented better classification performance than the other methods (99.69% for the overall accuracy and 0.9938 for the Kappa value).

These are essential inputs for refining the accuracy when great attention is required

for deriving this information from SAR imagery, to support better environmental monitoring and management of resources.

Keywords: Classification Techniques, Water Body Extraction, Terrasar-X Satellite, Imagery.

1. Introduction

Extraction of water bodies is an essential work in remote sensing and has been proved useful in many applications such as GIS database revision, flood forecasting and water resource management(Wang and Xie, 2018). This practice takes advantage of the data obtained from satellites and UAVs, which enables obtaining measurable information of water bodies that would not be accessible by traditional means(Acharya et al., 2021). At the same time, remote sensing approaches can be followed to monitor changes in water bodies over time, which improve the capability of researchers and decision- makers to understand environmental conditions and make effective decisions (Chen et al., 2022).

Remote sensing tools are applied using different apparatus to detect water, and they are able to give accurate information even in difficult weather conditions, heavy clouds or in the dark(Shareef et al., 2016). One of the most known instruments is Synthetic Aperture Radar (SAR), that can penetrate cloud and vegetation apparently used a longer wavelength. However, SAR encounters difficulty in differentiating water surface from non-water objects because of the existence of environmental factors such as wind speed, wind-induced waves or emergent vegetation that may disturb the smoothness of the water surface(Azeez et al., 2024).

To map water bodies, several classification techniques have been developed with remote sensing datasets. These methods can be broadly categorized into two types: single-band methods and multi-band methods(Shareef et al., 2020). In one band methods, a band from the multispectral image is selected for extracting the water

information. In multi-band approaches, the specular distinction between each contributing band is leveraged (Wang et al., 2024). This includes examining the spectral response of each ground target (i.e., water and land) and applying logical procedures (i.e., decision trees) to distinguish land and open water (Sharma et al., 2013).

The classification methodology ranges from sophisticated techniques like Artificial Neural Networks (ANN) and Support Vector Machines (SVM) to traditional algorithms like MLH, MHD, and MND (Saturi, 2023). Since pixel values in SAR data are discrete and occur within a specific interval, the MLH's underlying assumption that the data is regularly distributed may not hold true. On the other hand, recent techniques such as SVM and ANN provide a much higher classification accuracy as these techniques employ machine learning algorithms that can more effectively define classes in a way that is more precise and detailed (Ali et al., 2024).

Although there are numerous algorithms to extract water bodies based on remote sensing images, it is still difficult to detect water bodies from radar images from land feature, and especially to identify them when affected by environmental factors, such as wind or emergent vegetation (Bijeesh and Narasimhamurthy, 2020). This complicates the procedure of clearly drawing out water areas. The contribution of this research is in enhancing the accuracy of water body mapping through novel and advanced classification approaches, for the better promotion of the remote sensing techniques for environmental and planning resource management purposes (Shareef et al., 2015). Such a research will contribute to design new methods for both classification and processing feature signal to get the precise and confidence results to be used by researchers and governmental organizations to improve decision making in water resources and environment (Salahalden et al., 2024).

2. Methods

2.1 Data Used and the Study Area:

Stripmap (SM) mode TerraSAR-X HH-polarized images from 2013 were used in this study. TerraSAR-X satellite images provide high resolution data and are in the form of GeoTiff for compatibility with GIS. The images show the Atchafalaya Delta, a vibrant wetlands area in Louisiana in the southern United States (Inserra et al., 2023).

2.1.1 TerraSAR-X Specifications:

Polarization: The images are HH-polarized (H for horizontal transmit and H for horizontal receive) configuration, which is ideal for detecting water bodies, vegetation, and artificial structures.

Resolution: The spatial resolution of the photos is 3 m in slant range and 5 m in azimuth direction, which is a good enough to recognize small features such as water bodies or vegetation patterns (Werninghaus, 2004).

Incidence Angle: The incidence angle is 26.4°, which is important for the radar's senstivity to different surface types. This angle is optimal for obtaining surface-specific information, such as in areas with variable water levels such as wetlands.

Projection: We project the images on the TM (Transverse Mercator) projection including in the reference WGS 84 which offers that precise geographic location which is necessary for mapping and analysis (Pitz and Miller, 2010).

2.1.2 Study Area:

The image are all taken over the Atchafalaya Delta in Louisiana, which is one of the largest river deltas in the United States. The delta is the cumulative result of the confluence of the Mississippi and Atchafalaya Rivers and is celebrated for its vast network of marshes, swamps, and bayous.

This ecological-sensitive area is critically important as provides key habitat for many species of birds, fishes and plants. Its also valuable for flood control, water management, conservation and other purposes. The dynamic environment of the Delta, which is subject to water level and vegetation seasonality, makes it difficult to map and delineate water bodies with accuracy (Lane et al., 2018).

The information was recorded in 2013, which is a snapshot of the area at the time. Future imagery can also be compared with this historic data to monitor changes to the Delta, including alterations in the size of water bodies resulting from seasonal flooding or long-term climate change (Collins, 2015).

In general, the availability of TerraSAR-X HH-polarized images covering 2013 for Atchafalaya Delta, offers a unique opportunity to observe the complex water areas in this region. High-resolution images and methodologies for image classification but enough to support effective delineation, monitoring and management of the volume and flow of the Delta's waters can improve the optimum use of water resources and preservation of the environment (Sonobe et al., 2015).

Figure (1): Results of classifications by different classifiers

3. Advanced Classification Techniques and Limitations

3.1 Advanced Classification Techniques:

Artificial Neural Networks (ANNs), or just Neural Networks (NNs), have received much attention since the mid-eighties for the promising results obtained in supervised and unsupervised classification. Previous works have repeatedly reported that ANN-based algorithms outperformed the traditional classifier, e.g., MLH, especially in the remote sensing community (Thakur and Konde, 2021).

MLH comes from the Bayesian probability equation:

$$P(x,w) = P(w/x)P(x) = P(x/w)P(w) \quad (1)$$

The events are denoted by x and w. where P(w/x) is the conditional probability of event x occurring given event w, P(x, w) is the joint likelihood of events x and w occurring, and P(x) and P(w) are the prior probabilities of events.

A machine-learning method for modeling and quantifying intricate trends and phenomena, ANNs are a potent tool. They are made up of interconnected nodes, which are mathematical models that mimic the activity of the neurons. A neural network is a computational network consisting of many simple processing elements (nodes or units), loosely analogous to a biological neuron (Gurney, 1997). ANN are particularly useful in learning and predicting from data and can therefore be adjusted with greater precision, in contrast to linear predictions, in non-linear relationships and multiple, complex data.

Support vector machines (SVMs) have also gained much popularity in remote sensing image classification in long times. SVM is a supervised classification technique based on statistical learning theory. SVM is well suited for high-dimensional, noisy, complex data, and is extensively used for multi-dimensional data classification. What the SVM does is to look for the best hyperplane that

separates the points of different classes every time. When data are not linearly separable, SVM applies kernel tricks to project the input space into a higher-dimensional space so that the data can be better separated (Maulik and Chakraborty, 2017).

Mathematically, SVM aims to maximize the gap between two classes, which is given by:

Where the hyperplane can be written as:

$$w^T x + b = 0 \qquad (2)$$

Where b is the bias that establishes their position with respect to the origin, w is the normal to the hyperplane, and x is a point falling on the hyperplane. This indicates matrix transposition. Additionally, the origin is the Euclidean norm of w, and $|b|/\|w\|$ stands for the distance measured perpendicularly from the hyperplane(Amer et al., 2024).

3.2 Limitations of Classification Techniques:

Though the classical methods such as MLH occasionally obtain above 80% of the accuracy, it requires that data set to be normally distributed which can be seen as a limitation (Pal and Mather, 2001). (Foody, 1999) noted that standard statistical methods might not necessarily be appropriate for mapping with remote sensing, and this is especially the case when combining multiple datasets from different sources.

To be specific, MLH assumes the data of each class have the same Gaussian distribution, however, this assumption could not always hold on for the remote sensing data. Pixel values of SAR data are discrete and range-limited, for which the normality assumption becomes unrealistic. MLH needs a large number of training data to define typical samples for all classes. On the basis of Mather (Pal

and Mather, 2001), the minimum number of observations that should be used as a training set is 10-30 times the number of discriminating as predictions. This is a difficulty, and becomes a problem when we look at extrapolation across large areas with sparse ground data.

Based on such a distribution assumption, the Mahalanobis Distance (MHD) and Minimum Distance (MND) approaches are developed, however, such assumptions are often difficult to satisfy in practice, as the data of each class may not be elliptically shaped in feature space. Where the Mahalanobis distance is as follows: MND uses the Euclidean distance to classify the pixels supposing equal variance and no correlation between features. One consequence is that the resulting clusters tend to be round and this may be ambiguous when the means of two classes are close to each other (Younis, 1996).

Although NNs can achieve superior classification accuracies compared to classical classifiers, they are usually not statistically solid, and do not yield direct estimates of uncertainty (Gawlikowski et al., 2023). In MLH, probability maps can represent how reliable a pixel is for an assignment to a specific class, a feature for which (most) NNs do not provide easy access. If the network becomes too complicated or if the training data is too scarce, NNs can also have a problem with overfitting, which results in poor generalization to new data (Abdulrahman et al., 2024).

On the other hand, SVM is insensitive and performs well for smaller data sets unlike other classifiers. It also works well when the data is noisy or when there are outliers in the data. Moreover, SVM is based on a solid mathematical basis, which is more stable and explainable (Maarez et al., 2022). Limitations of SVM require transforming the problem into a binary classification to be solved by SVM classifier, and thus is limited to multiple-class problems. And the training time can be time consuming, especially on a large dataset. Moreover, the search for the best hyperplane is complicated by the fact that it works in a high-dimensional space

resulting from non-linear reparability (Hasan et al., 2024).

4. The Accuracy Assessment of the Classified Images

A confusion matrix or error matrix can be used to assess classification accuracy. The array is square n x n, where n is the number of classes. Typically, the matrix displays the classifier's assigned class in rows and the class label in columns for evaluation data. The total accuracy, user and producer accuracy, Kappa coefficient, and conditional Kappa are often used classification accuracies (Fahmy Amin, 2023). The confusion matrix serves as the foundation for these statistics. Let the number of samples classified as belonging to category using remote sensing data is expressed as More specifically, the expression of using remote sensing data will be expressed as:

$$n_{i+} = \sum_{j=1}^{k} n_{ij} \qquad (3)$$

Additionally, the reference data set's number of samples categorized into category j can be written as

$$n_{+j} = \sum_{i=1}^{k} n_{ij} \qquad (4)$$

Therefore, the following formula can be used to determine the overall accuracy between the reference data and the remotely sensed classification.

$$\text{Overall accuracy} = \frac{\sum_{i=1}^{k} n_{ii}}{n} \qquad (5)$$

where n is the total number of evaluation pixels and nii is the sum of the diagonal entries of the matrix, or correctly categorized pixels. Furthermore, the likelihood that the classified image is accurate is represented by the overall accuracy. Additionally, the confusion matrix's producers' accuracy is determined by dividing the number of correctly identified class pixels by the entire amount of evaluation pixels for that

class (column total)(Noori et al., 2018).

$$\text{Producer's accuracy } j = \frac{n_{ii}}{n_{+j}} \quad (6)$$

The ratio of pixels correctly classified as the j-th class to the total number of pixels classified by the classifier for the j-th class (represented by the confusion matrix's row total) indicates the user's accuracy. The parties can then express the user's accuracy:

$$\text{User's accuracy } i = \frac{n_{ii}}{n_{i+}} \quad (7)$$

It is important to note that for each class in the categorized image, the accuracy of the user and the producer produces the impression of the commission mistake and the omission error, respectively (Salahalden et al., 2023).

Errors of commission can be referring to pixels from other classes that the classification technique has labelled as belonging to the class of interest. Therefore, the commission error of class i, and calculated by:

$$\text{Commission error } = 1 - \frac{n_{ii}}{n_{i+}} \quad (8)$$

Whereas, the errors of omission are defined by pixels who's belonging to the class of interest (ground truth) that the classifier has failed to classify them into the proper class then the omission error of class ^{j}, can be given by

$$\text{Omission errors } = 1 - \frac{n_{ii}}{n_{+j}} \quad (9)$$

The kappa coefficient measures the degree of similarity between the classified image and the evaluation data(Jaber et al., 2022). The equation is

$$K = \frac{n\sum_{i=1}^{k} n_{ii} - \sum_{i=1}^{k}\left(n_{i+} \times n_{+j}\right)}{n^2 - \sum_{i=1}^{k}\left(n_{i+} \times n_{+j}\right)} \quad (10)$$

The equation's variables are as follows: k is the number of rows in the matrix of confusion; ni+ and n+j are the row and column sums of the individual classes; nii are the correctly classified pixels of classes (entries in the principal diagonal); and is the total count of the evaluation pixels. The following formula states that the kappa coefficient ranges from -1 to +1; the higher the number, the better the categorization for calculating the kappa coefficient quality standard, which is provided in Table 1.

Table (1): Classification quality related to the values of the kappa coefficient

Kappa Value	Quality
<0.00	Worst
0.00-20	Poor
21-40	Reasonable
41-60	Good
61-80	Very good
81-100	Excellent

5. Result and Discussion

5.1 Classification by Different Methods:

From the analysis of the training data, three main categories were separated: Water bodies and Land use and Land cover. These categories were classified with five methods: MLH, MHD, MND, NN, and SVM. These classified maps were then assessed visually and accuracy assessment metrics previously mentioned were used to assess the results of these classifications.

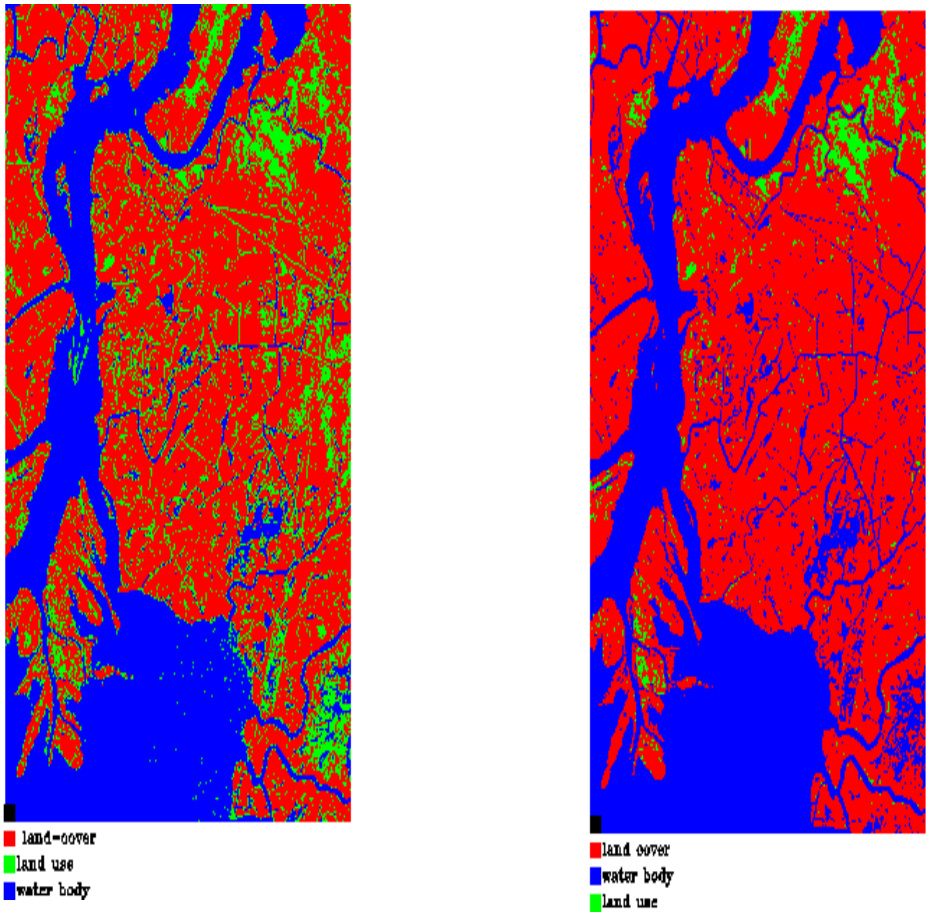

MLH MND

Figure (2): Classification outcomes from several classifiers MLH, MND

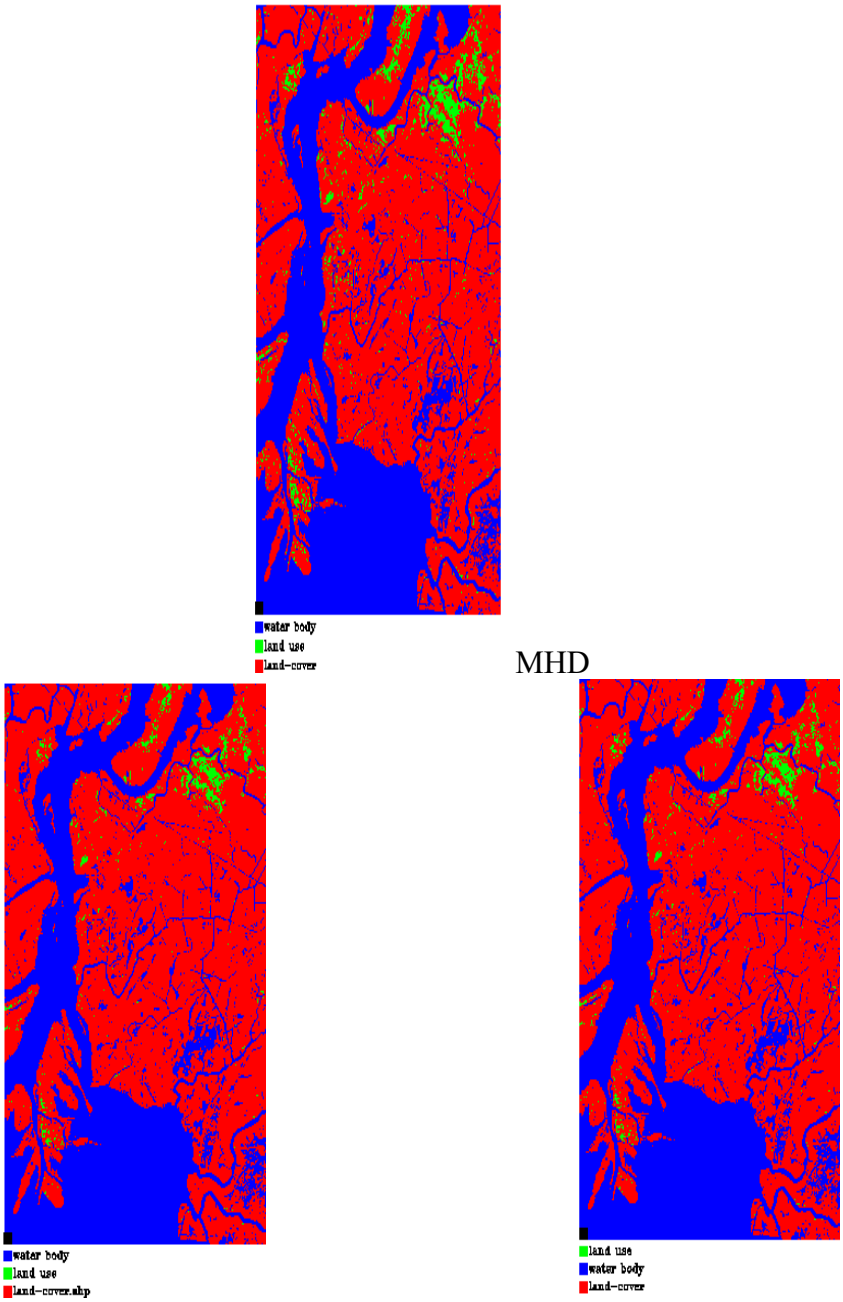

Figure (3): Results of classifications by different classifiers MHD, ANN, SVM

International Journal for Scientific Research, London Vol (4), No (7), 2025
https://doi.org/10.59992/IJSR.2025.v4n7p15 E-ISSN 2755-3418

Through a visual examination of Figure 2, it can be seen that the land cover (visualised in red) and land use (visualised in green) are frequently overlapped within the MLH image, and water body areas (visualised in the blue) have been misclassified as land cover throughout large sections of the image. Moreover, there are a couple of evident cases where land use is erroneously spread to water body regions in several image locations.

In Figure 3 which contains the MHD image, the land cover, land use and water body classes are also mingled with each other. However, in this case, the misclassification is dominated by water bodies, creating particular difficulties in certain regions.

The MND image also shows a similar condition as the MHD image with an analogous combination of land cover, land use and water body classes. This could be interpreted as a lack of discriminative capability of the classification methods we have applied to these classes.

In comparison, mixing of land use and land cover can be seen to be significantly lower when applying the NN approach. Although there is a small amount of overlap, it is significantly smaller than that from MLH, MHD, and MND. In addition, water body areas are clearly outlined and there were no areas affected by misclassification which indicates that NN is able to classify these areas more raster con accurateness.

In the support vector machine image classes land cover, land use and water body are well separable and the error is not as severe. The water body regions in particular are more distinct in the SVM image than for results from MLH, MHD and MND. Furthermore, the conjugation of LU and LC is markedly weakened, thereby indicating that SVM is superior in getting class separation and clarity.

In summary, the service of the NN and SVM are much better than the MLH, MHD and MND in terms of the classification accuracy especially for the water body areas and the decrease of class entropy. The separations are the best for the distribution pattern by the SVM method and smallest misclassification.

5.2 The Accuracy of Image Classification:

The classified scenes were compared to the reference data to obtain confusion matrices which show the comparison of the actual field scene and the predicted class from the different methods applied in this research. A part of the captured field recordings were reserved as test data as reported previously. The confusion matrices, shown in Table 2, indicate how the predicted and actual classifications of each class are related. Rows labelled as "Column Total" indicate the total amount of pixels available for the given class in consideration. It is evident from these matrices, that the water body class is the most separable in all classification methods, which is a typical finding when it comes to remote sensing image classification.

In general, all methods were successful in identifying the water body areas. Nonetheless, the MLH method resulted in considerable misclassification with a majority (land cover and land use) of most classes misclassified as the water body class. As a consequence, land cover/land use classes partially overlap on water bodies, which in turn introduce errors in the classification accuracy.

The misclassification between land cover and land use categories is a common problem for all methods, apart from the SVM algorithms. In the SVM, although misclassification is somewhat reduced, but there is still some overlap between land use and land cover classes. Such an overlap results from the fact that land use and land cover frequently use similar land types and have closely associated spectral properties, particularly in time–series SAR images (see Figure 2).

The MLH and MHD show severe confusion between land covers and land uses. This misgeneralization and cross-contamination between the two sets of the samples engenders the difficulty of properly discrimating them. Likewise, the Minimum Nearest Distance (MND) also has similar behavior to the MHD with incorrect classification and overlapping in the land cover and land use classes. This is also observed in the confusion matrices that there are small differences of the classification of land use and land cover compared to the class of water body.

The NN technique performs marginally better as it is able to get back some misclassified pixels of the land cover class(s) from the water body class. But it continues to make many errors of commission in classifying land cover pixels including some salt water body class pixels which show the omission error. The waterrclass used in the NN method is heavily misclassified as terrain cover because of the similar spectral characteristics of the terrain cover and water. Furthermore, landuse covers with landcover of the same type in a lot of places across the study region which contributes to the complications between the latter and the former class.

The SVM model, however, proved to be the most precise model to the current research. The classes are not interacting at all, there are no false positives. SVM also achieves an outstanding distinction between the classes of land cover, land use, and water body, as demonstrated in the confusion matrix. No misclassification and low overlap between classes, makes SVM the most appropriate method for this classification.

Overall, the techniques MLH, MHD and MND demonstrate a significant amount of misclassification and their classes overlap. Yet SVM gives the most accurate and precise ones. The water body class is well separated with all methods, but if we want to use single only one model for all classes to perform a multi-class

classification, then the SVM highest multidimensional separation between LU/LC and water body, we hence opt for it in this study.

5.3 Evaluation of Classifier Performance:

Table 2 displays the confusion matrix results, which include the overall accuracy and Kappa coefficients for the various approaches. To assess the usefulness of each approach, these values are then calculated for every classified image. The degree of agreement between the classification and field identification is shown by the Kappa coefficient, while the total accuracy indicates how accurate the categorized image is. The commission error, or the proportion of pixels from classes other than the one in issue that have been incorrectly classified as that class, represents the user's accuracy. The commission error decreases as user accuracy increases. In the correspondence, the omission error—that is, the percentage of pixels labelled as various classes that you wish to classify as the present class—corresponds to the producer's accuracy. There is less omission error the more accurate the producer is. More information is provided by the Kappa coefficient, which takes into account both the accuracy of the producer and the user. It is a universal feature of the classification's quality.

Table (2): Calculated confusion matrix in relation to field data

Method	Class	land-cover	Land use	Water body	Total	Kappa Coefficient	Over all Accuracy
Maximum likelyhood	land-cover	46000	0	800	46800	0.7594	85.7300%
	Land use	7131	1678	4638	13447		
	Water body	0	0	27833	27833		
	Total	11731	1678	33271	88080		
Mahalonobis distance	land-cover	52600	0	16	52616	0.9700	98.5070%
	Land use	1315	848	830	2993		
	Water body	0	0	32471	32471		
	Total	53915	848	33317	88080		
Minimum Distance	land-cover	52600	0	16	52616	0.9700	98.5070%
	Land use	1315	841	837	2993		
	Water body	0	0	32471	32471		
	Total	53915	841	33322	88080		
Neural network	land-cover	53931	178	197	54306	0.9913	99.5743%
	Land use	0	1500	0	1500		
	Water body	0	0	32274	32274		
	Total	53931	1678	32471	88080		
Supported vector machine	land-cover	53859	0	197	54056	0.9938	99.6946%
	Land use	72	1678	0	1750		
	Water body	0		32274	32274		
	Total	53931	1678	32471	88080		

A global view of classification is provided by the global measurements of accuracy and the Kappa coefficient. According to Table 3, the NN and SVM perform better than the MLH, MHD, and MND approaches, displaying the best levels of overall accuracy and Kappa coefficient. The best classifier in this study is the SVM approach, which has the highest overall accuracy of 99.69% and the Kappa coefficient of 0.9938.

Table (3): Classifier accuracy and Kappa coefficients

Classifier	MLH	MHD	MND	NN	SVM
Overall Accuracy	86.6383%	98.5070%	98.5070%	99.5743%	99.6946%
Kappa coefficient	0.7594	0.9700	0.9700	0.9913	0.9938

SVM works better, as shown by the producer's and user's accuracy results, which are shown in Table 4. With the MLH approach, the user's accuracy for the land cover class is very low (85.72%), but with the SVM method, the producer's and user's accuracy for every other class is almost flawless, indicating its robustness in reducing commission and omission errors. This demonstrates that SVM is efficient in both classifying pixels from other classes (low commission error) and pixels from each class (low omission error).

Table (4): Accuracy of users and producers

User's accuracy (%)					Classes	Producer's accuracy (%)				
MLH	MHD	MND	NN	SVM		MLH	MHD	MND	NN	SVM
85.72	100.00	100.00	99.39	99.39	Water body	100.00	100.00	100.00	100.00	100.00

The SVM approach yields higher detection rates, Kappa and fewer misclassifications than other classification methods. The NN method also exhibits good performance; however, in identifying the land use-land cover-water body classes, SVM shows a greater accuracy in classification, specifically.

6. Conclusion

In this paper, various classification algorithms were evaluated in the context of water body extraction from TerraSAR-X images in the Atchafalaya Delta in LA. The outcomes indicated that the max likelihood classification (MLH), MHD and MND methods were not efficient to process and classify the vegetation cover, since their levels of misclassification were large, in which errors occurred where water features were confused with terrestrial features.

However, comparison results of NN and SVM using advanced methods were

reported with a high classification accuracy. SVM in particular showed the optimal performance with an accuracy of 99.69% and Kappa value of 0.9938, providing a more precise classification of water bodies and land classes.

These findings suggest that applying machine learning methods, such as SVM and NN could be used to increase the accuracy of remote sensing classification, especially in difficult terrain types like wetlands. These more advanced methods give a more accurate result and are necessary for environmental monitoring and resource management applications.

References

- ABDULRAHMAN, M. I., SHAREEF, M. A. & AL-ATTAR, A. A. 2024. Deep Learning (CNN) for Detecting Road Infrastructure in Old Mosul City Using High-Resolution Aerial Imagery. *Baghdad Science Journal*.
- ACHARYA, B. S., BHANDARI, M., BANDINI, F., PIZARRO, A., PERKS, M., JOSHI, D. R., WANG, S., DOGWILER, T., RAY, R. L. & KHAREL, G. 2021. Unmanned aerial vehicles in hydrology and water management: Applications, challenges, and perspectives. *Water Resources Research,* 57**,** e2021WR029925.
- ALI, C. A., SHAREEF, M. A. S. & AL NUAIMY, Q. A. 2024. Estimating Soil Parameters Using C Band Synthetic Aperture Radar in Laylan, Iraq. *Ecological Engineering & Environmental Technology,* 25.
- AMER, A., ALHADITHI, M. & SHAREEF, M. A. Creating landslide susceptibility map using frequency ratio (FR) model in Soran city, Irbil Province, Iraq. AIP Conference Proceedings, 2024. AIP Publishing.
- AZEEZ, S. M., SHAREEF, M. A. & OMER, F. M. 2024. Eco-Environmental Quality Assessment of Two Seasons Based on Pressure-State-Response Framework by Using Remote Sensing and GIS Techniques. *The Iraqi Geological Journal***,** 233-252.
- BIJEESH, T. & NARASIMHAMURTHY, K. 2020. Surface water detection and delineation using remote sensing images: A review of methods and algorithms. *Sustainable Water Resources Management,* 6**,** 68.

- CHEN, J., CHEN, S., FU, R., LI, D., JIANG, H., WANG, C., PENG, Y., JIA, K. & HICKS, B. J. 2022. Remote sensing big data for water environment monitoring: Current status, challenges, and future prospects. *Earth's Future,* 10**,** e2021EF002289.
- COLLINS, J. 2015. *Defining the Delta: Multidisciplinary Perspectives on the Lower Mississippi River Delta*, University of Arkansas Press.
- FAHMY AMIN, M. 2023. Confusion matrix in three-class classification problems: A step-by-step tutorial. *Journal of Engineering Research,* 7**,** 0-0.
- FOODY, G. M. 1999. The continuum of classification fuzziness in thematic mapping. *Photogrammetric engineering and remote sensing,* 65**,** 443-452.
- GAWLIKOWSKI, J., TASSI, C. R. N., ALI, M., LEE, J., HUMT, M., FENG, J., KRUSPE, A., TRIEBEL, R., JUNG, P. & ROSCHER, R. 2023. A survey of uncertainty in deep neural networks. *Artificial Intelligence Review,* 56**,** 1513-1589.
- GURNEY, J. R. 1997. An investigation into children's developing mathematical abilities.
- HASAN, S. F., SHAREEF, M. A. & JABER, H. S. 2024. Influence of Noise Equivalent Beta Naught estimation on backscattering image classification of TerraSAR-X. *Geodesy and Cartography,* 50**,** 104–112-104–112.
- INSERRA, G., BUONO, A., NUNZIATA, F., VIRELLI, M. & MIGLIACCIO, M. 2023. On the extraction of the reservoirs' waterline using polarimetric X-band SAR measurements: the case study of the San Giuliano reservoir, Italy. *International Journal of Remote Sensing,* 44**,** 6060-6088.
- JABER, H. S., SHAREEF, M. A. & MERZAH, Z. F. 2022. Object-based approaches for land use-land cover classification using high resolution quick bird satellite imagery (a case study: Kerbela, Iraq). *Geodesy and Cartography,* 48**,** 85-91.
- LANE, R. R., PAUL KEMP, G. & DAY, J. W. 2018. A brief history of delta formation and deterioration. *Mississippi Delta Restoration: Pathways to a sustainable future***,** 11-27.
- MAAREZ, H. G., JABER, H. S. & SHAREEF, M. A. 2022. Utilization of Geographic Information System for hydrological analyses: A case study of Karbala province, Iraq. *Iraqi Journal of Science***,** 4118-4130.
- MAULIK, U. & CHAKRABORTY, D. 2017. Remote Sensing Image Classification: A survey of support-vector-machine-based advanced techniques. *IEEE Geoscience and Remote Sensing Magazine,* 5**,** 33-52.

- NOORI, A. M., HASAN, S. F., AJAJ, Q. M., MEZAAL, M. R., SHAFRI, H. & SHAREEF, M. 2018. Fusion of Airborne Hyperspectral and WorldView2 Multispectral Images for Detailed Urban Land Cover Classification A case Study of Kuala Lumpur Malaysia. *International Journal of Engineering Technology,* 7**,** 202-206.
- PAL, M. & MATHER, P. M. Decision tree based classification of remotely sensed data. 22nd Asian conference on remote Sensing, 2001. 9.
- PITZ, W. & MILLER, D. 2010. The terrasar-x satellite. *IEEE Transactions on Geoscience and Remote Sensing,* 48**,** 615-622.
- SALAHALDEN, V. F., SHAREEF, M. A. & AL NUAIMY, Q. A. 2023. Characterization of the chemical properties of deposited red clay soil using GIS based inverse distance weighted method in Kirkuk City, Iraq. *Ecological Engineering & Environmental Technology,* 24.
- SALAHALDEN, V. F., SHAREEF, M. A. & AL NUAIMY, Q. A. 2024. Estimation of red clay soil in Kirkuk City using Satellite remote sensing data. *NTU Journal of Engineering and Technology,* 3.
- SATURI, S. 2023. Review on machine learning techniques for medical data classification and disease diagnosis. *Regenerative Engineering and Translational Medicine,* 9**,** 141-164.
- SHAREEF, M., HASSAN, N., HASAN, S. & KHENCHAF, A. 2020. Integration of Sentinel-1A and Sentinel-2B data for land use and land cover mapping of the Kirkuk Governorate, Iraq. *International Journal of Geoinformatics,* 16**,** 87-96.
- SHAREEF, M. A., KHENCHAF, A. & TOUMI, A. Integration of passive and active microwave remote sensing to estimate water quality parameters. 2016 IEEE Radar Conference (RadarConf), 2016. IEEE, 1-4.
- SHAREEF, M. A., TOUMI, A. & KHENCHAF, A. Estimation and characterization of physical and inorganic chemical indicators of water quality by using SAR images. SAR Image Analysis, Modeling, and Techniques XV, 2015. SPIE, 140-150.
- SHARMA, R., GHOSH, A. & JOSHI, P. 2013. Decision tree approach for classification of remotely sensed satellite data using open source support. *Journal of Earth System Science,* 122**,** 1237-1247.
- SONOBE, R., TANI, H., WANG, X., KOBAYASHI, N. & SHIMAMURA, H. 2015. Discrimination of crop types with TerraSAR-X-derived information. *Physics and Chemistry of the Earth, Parts A/B/C,* 83**,** 2-13.

- THAKUR, A. & KONDE, A. 2021. Fundamentals of neural networks. *International Journal for Research in Applied Science and Engineering Technology,* 9**,** 407-426.
- WANG, X. & XIE, H. 2018. A review on applications of remote sensing and geographic information systems (GIS) in water resources and flood risk management. *Water,* 10**,** 608.
- WANG, Z., WANG, X., LI, G. & WU, W. MBF: A Multi-Band Fusion Method for Sandy Water Extent Mapping Based on Multispectral Satellite Images. IGARSS 2024-2024 IEEE International Geoscience and Remote Sensing Symposium, 2024. IEEE, 9778-9781.
- WERNINGHAUS, R. TerraSAR-X mission. SAR image analysis, modeling, and techniques VI, 2004. SPIE, 9-16.
- YOUNIS, K. S. 1996. Weighted Mahalanobis distance for hyper-ellipsoidal clustering.